

## Photoluminescence studies of indirect bound excitons in $\epsilon$ -GaSe

Y. Sasaki\* and Y. Nishina

*The Research Institute for Iron, Steel, and Other Metals, Tohoku University, Sendai 980, Japan*

(Received 17 November 1980)

The binding centers of the indirect bound excitons in  $\epsilon$ -GaSe are identified from the magnetoluminescence up to 10 T at 4.2 K and from the temperature dependence of the photoluminescence spectra in the temperature range from 4.2 to 25 K. The two different kinds of experiments lead to the same conclusion that six indirect bound-exciton lines in the photon energy range of 2.0785 to 2.0992 eV at 4.2 K are due to the radiative recombination of ionized-donor exciton complexes. The valley-orbit state of the donor is  $A_1$  or  $A_2$  in the site symmetry of  $C_{3v}$  or  $D_{3h}$ , respectively. The observed photoluminescence lines are spin-triplet states of the bound exciton partially mixed with the singlet component by the spin-orbit interaction. The effective  $g$  values of the hole and donor electron are  $|g_{e\parallel} + g_{h\parallel}| = 3.65 \pm 0.1$  and  $|g_{e\perp} + g_{h\perp}| = 3.23 \pm 0.15$ , where  $\parallel$  or  $\perp$  indicates the magnetic field direction with respect to the crystal  $c$  axis. These  $g$  values are identical throughout the six indirect bound-exciton lines studied here. The temperature dependences of the photoluminescence spectra give estimation of the ionization energies of the donor as 40 to 55 meV, and the binding energy of the hole to a neutral donor as about 10% of these ionization energies.

### I. INTRODUCTION

The photoluminescence (PL) spectrum of layer compound GaSe below about 10 K is characterized by many sharp lines.<sup>1</sup> There has been a considerable degree of inconsistency in the assignments of these PL lines in the literature because of the spectral complexity. The three kinds of PL lines have been identified in the PL spectra of  $\epsilon$ -GaSe below 10 K (Refs. 1 and 2): (1) the direct free exciton (DFE) lines observed in the photon energy range between 2.105 and 2.113 eV, where the stacking fault induces the line splitting, (2) direct bound-exciton (DBE) lines between 2.100 and 2.105 eV, and (3) indirect bound-exciton (IBE) lines and their phonon replicas between 2.047 and 2.0995 eV. Very few of the reports in the past, however, deal with the nature of binding centers of these bound excitons. The coexistence of DBE and IBE is due to the band structure peculiar to  $\epsilon$ -GaSe; i.e., the direct and indirect band gaps are almost equal<sup>2,3</sup> within the energy difference of 10 meV or so.

In general, it is rather unusual that the conventional PL experiment can clarify the nature of the binding center of bound excitons in detail. Splittings of the bound states by an application of external perturbation may give precise information for the study of the bound states. Magnetic field is one of the most useful perturbations for the identification of the bound-exciton state.<sup>4</sup> Recent experiments of the magnetoluminescence of GaSe suggest that the IBE states responsible for PL at low temperatures are triplet.<sup>5-7</sup>

This paper reports the magnetoluminescence spectra up to 10 T and the temperature dependence of the PL spectra in GaSe in order to identify the electronic state of the binding center

of IBE. In Sec. II the band structure of GaSe is explained, and the experimental procedures are stated in Sec. III. Section IV describes the Zeeman spectra of the IBE lines in the Faraday and Voigt configurations, and the thermal quenching of the IBE lines. The angular dependence of the Zeeman splitting is also given. In Sec. V the electronic state of the binding center responsible for the IBE lines is deduced from the Zeeman spectra and the thermal quenching data of the IBE lines. The experimental results of the Zeeman spectra are compared with the theoretical predictions for ionized- and neutral-impurity exciton complexes. Preliminary results of the present study have been reported in Ref. 6.

### II. BAND STRUCTURE OF GaSe NEAR THE ABSORPTION EDGE

Our analysis of the Zeeman data is based on the near-edge band structure as explained in the following. The direct band gap of  $\epsilon$ -GaSe ( $D_{3h}$ ) is located at the  $\Gamma$  point with its energy of 2.129 eV at 4.2 K.<sup>8</sup> In the higher photon energy region there have been several reports regarding structures in reflectance,<sup>9</sup> electroreflectance,<sup>10</sup> and ellipsometric measurements.<sup>11</sup> The second-lowest band edge in energy is observed at 3.38 eV at 77 K (or 3.23 eV at 300 K), and it is allowed for  $\vec{E} \perp c$  but may be forbidden for  $\vec{E} \parallel c$ ,<sup>11</sup> where  $\vec{E}$  and  $c$  denote the electric field vector of light and the crystal  $c$  axis, respectively. The type of this critical point is assigned as  $M_0$  type and the interband reduced mass is estimated to be about  $0.1m_0$  with some anisotropy.<sup>9,10</sup> The critical point at 3.70 eV at 77 K has been assigned as the spin-orbit split-off pair of the 3.38 eV critical point from the analysis of the electroreflectance

spectra.<sup>10,12</sup> Following Schlüter's calculation,<sup>9,13</sup> the top of the valence and the bottom of the conduction bands at the  $\Gamma$  point have the symmetry of  $\Gamma_1^v$  and  $\Gamma_4^c$  in the notation of Koster *et al.*,<sup>14</sup> where the superscripts  $v$  and  $c$  denote the valence and conduction bands, respectively. The selection rule deduced from the band structure and the ellipsometric measurement suggests that the structures at 3.38 and 3.70 eV are due to the transitions to the  $\Gamma_4^c$  band from the  $\Gamma_5^v$  band with Se  $p_{x,y}$ -like character, which splits into  $\Gamma_7^v$  and  $\Gamma_9^v$  by the spin-orbit interaction. Consequently, these valence and conduction bands are not degenerate at the band edges. Figure 1 shows the band model of  $\epsilon$ -GaSe around 4.2 K with modification in energy from the result of Schlüter in order to fit the experimental results of reflectance,<sup>9</sup> electroreflectance,<sup>10</sup> and PL spectra.<sup>3</sup> The band-edge energies for  $\Gamma_5^v$ - $\Gamma_4^c$  and  $\Gamma_7^v$ - $\Gamma_4^c$  are higher in Fig. 1 by 0.03 eV than those in Ref. 10, taking into account the binding energy of the exciton and the shift of the band edge by temperature variation.

The optical transition in the vicinity of the direct edge is allowed in  $\vec{E} \parallel c$ , but the transition probability for  $\vec{E} \perp c$  is weaker by a factor of  $10^{-2}$  than in  $\vec{E} \parallel c$ . The  $\vec{E} \perp c$  component is attributed to the intervalence-band mixing between the  $\Gamma_1^v$  and  $\Gamma_5^v$  bands by the spin-orbit interaction. The ratio of the oscillator strength for  $\vec{E} \perp c$  and  $\vec{E} \parallel c$  suggests that about 10% of the  $\Gamma_5^v$  component mixes with  $\Gamma_1^v$ . The degree of mixing is reasonable in the light of the quasicubic model applied to GaSe,<sup>15</sup> where the  $\Gamma_1^v$  and  $\Gamma_5^v$  bands consist of the  $p_x$  and  $p_{x,y}$  orbit of Se, respectively.

The indirect absorption edge consists of a  $\Gamma_1^v$ -

$M_2^c$  band pair.<sup>9,13</sup> Since the direct and indirect edges are very close to each other, it has been very difficult to determine the energy of the indirect edge. Recently, the indirect exciton energy for  $\epsilon$ -GaSe ( $2.100 \pm 0.002$  eV) and  $\gamma$ -GaSe ( $2.089 \pm 0.002$  eV) has been determined by the extrapolation from GaSe<sub>1-x</sub>S<sub>x</sub> mixed crystals of  $0.01 \leq x \leq 1$  to  $x=0$ .<sup>3</sup> The binding energy of the indirect exciton,  $\approx 40$  meV, has been deduced from the gain coefficient curve analysis of the stimulated emission in  $\epsilon$ -GaSe.<sup>16</sup> The indirect-gap energy of 2.140 eV is deduced from these results for  $\epsilon$ -GaSe. It should be noted that the indirect conduction-band edge is  $\approx 10$  meV higher than the direct one. Our model indicates that the conduction-band minimum is at the  $\Gamma$  point but the exciton gap shows a minimum at the  $M$  point.

Mercier, Mooser, and Voitchofsky<sup>17</sup> report, on the other hand, that the indirect band gap is 2.103 eV, and Thanh and Depeursinge<sup>18</sup> indicate that the exciton edge is 2.075 eV at 1.8 K. If their band scheme were correct, the luminescence lines above 2.075 eV (equal to indirect exciton edge of their band model) would have a very short lifetime because the bound excitons responsible for such luminescence lines can relax to the indirect exciton rapidly. Experimentally, the lifetimes of most of the PL lines below 2.100 eV are about  $10^{-6}$  sec, while they are shorter than  $10^{-8}$  sec for the lines above this energy.<sup>2</sup> The structures, therefore, in the optical-absorption spectrum of GaSe below the direct exciton reported by Thanh and Depeursinge may not be due to the indirect exciton but to some kind of impurities or defects. The threshold in the lifetime of the luminescence lines at about 2.100 eV (Ref. 2) agrees with the indirect exciton energy of our model shown in Fig. 1.

### III. EXPERIMENTAL ARRANGEMENTS

The single crystals of GaSe were grown by the Bridgman method with 99.999% Ga and Se as the source materials and without doping. The crystals were identified as  $\epsilon$ -GaSe by the x-ray analysis. They were always found as  $p$  type with  $N_A - N_D \approx 10^{15}$  cm<sup>-3</sup> and  $N_A + N_D \approx 10^{17}$  cm<sup>-3</sup>, where  $N_A$  and  $N_D$  were concentrations of acceptors and donors, respectively. In the PL experiments, the freshly cleaved surface was excited by the 488-nm line of an Ar-ion laser (50 mW at maximum), and the luminescence from the excited spot was focused on the entrance slit of a 75-cm double-grating monochromator (Nalumi 750Z-1200). The light was detected by a GaAs photocathode photomultiplier (Hamamatsu R-636). A typical resolution in the present measurements was 0.3 meV.

The magnetoluminescence experiment was

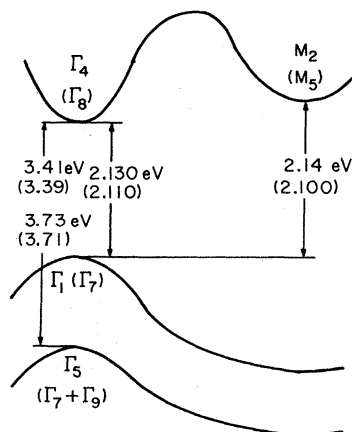


FIG. 1. Electronic band model of  $\epsilon$ -GaSe at 4.2 K near the  $\Gamma$  and  $M$  points. The notations in the parentheses are the double-group representation. The energies of the exciton ground states are given in the parentheses.

performed with the use of a 10-T split-type superconducting magnet. The luminescence spectra for an arbitrary angle,  $\theta_H$ , could be taken by the rotation of the sample, where  $\theta_H$  was the angle between the magnetic field  $\vec{H}$  and the  $c$  axis. The temperature dependence of the PL spectrum was measured with the use of a helium-gas-cooled cryostat, where the excitation power was less than 3 mW.

#### IV. RESULTS

The typical PL spectrum of undoped  $\epsilon$ -GaSe is shown in Fig. 2, where the assignment of the lines is as follows: (1) DFE lines are the luminescence from DFE triplet states,<sup>1</sup> where the line splitting is due to the stacking fault. (2)  $I_i$  ( $i=1$  to 5) lines are due to the annihilation of IBE without phonon assistance.<sup>19</sup> (3)  $I_i$ -MC lines are the momentum-conserving phonon replica of the  $I_i$  lines.<sup>3,19</sup> (4) The other lines may be due to DBE (Ref. 1) or transition of free carrier to an impurity bound state.

##### A. Zeeman spectra

Figure 3 shows the Zeeman spectra of the  $I_5$  line in the Faraday configuration with  $\vec{H} \parallel c$  and in the Voigt with  $\vec{H} \perp c$ , where the monotonous background in the luminescence spectra has been subtracted. In the Faraday configuration with  $\vec{H} \parallel c$ , the  $I_5$  line split into two and they are circularly polarized. The line at the lower-energy side is stronger than the at the higher side, and the ratio of these line intensities increases with the applied magnetic field due to the thermalization between the split states. The degree of circular polarization,

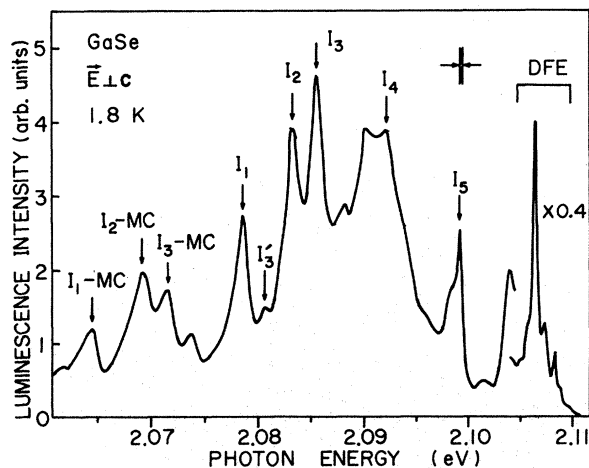


FIG. 2. Photoluminescence spectrum of  $\epsilon$ -GaSe at 1.8 K measured for  $\vec{E} \perp c$ .

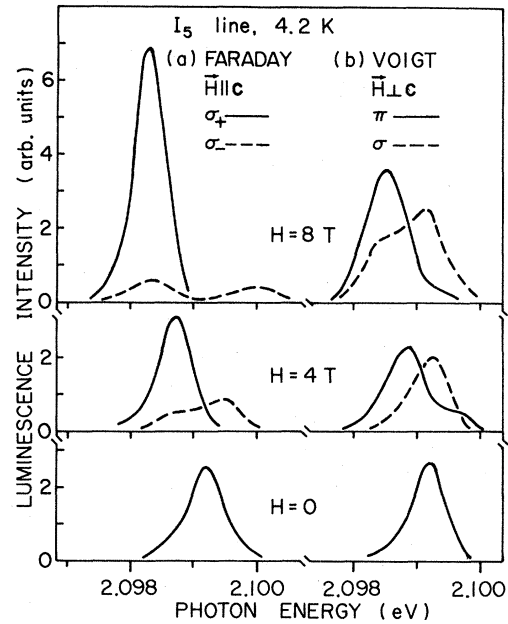


FIG. 3. Magnetoluminescence spectrum of the  $I_5$  line for (a) the Faraday and (b) Voigt configurations obtained at 4.2 K. The monotonous background has been subtracted for simplicity. Similar results have been obtained for all the  $I_i$  lines and their phonon replicas.

$$\rho_c = [I(+)-I(-)]/[I(+)+I(-)],$$

of the line at the lower-energy side is about 0.8 for  $H \geq 2$  T, where  $I(+)$  or  $I(-)$  is the intensity for the  $\sigma_+$  or  $\sigma_-$  circular polarization, respectively. In the Voigt configuration with  $\vec{H} \perp c$ , on the other hand, the  $I_5$  line splits into three; one is polarized for  $\vec{E} \perp \vec{H}$  ( $\sigma$  polarization), which shows no energy shift, and the other two for  $\vec{E} \parallel \vec{H}$  ( $\pi$  polarization). It may be noted here that  $\vec{E}$  is always normal to the  $c$  axis in the present experiments. The line observed at higher-energy side in the  $\pi$  polarization is not resolved at 8 T due to the thermalization among the split states. The degree of the linear polarization,

$$\rho_l = [I(\pi) - I(\sigma)]/[I(\pi) + I(\sigma)],$$

is estimated to be  $|\rho_l| \approx 0.5$  for  $H \geq 4$  T, where  $I(\pi)$  or  $I(\sigma)$  is the intensity for  $\pi$  or  $\sigma$  polarization, respectively. The Zeeman spectra of the other  $I_i$  lines and their phonon replicas are identical to that of the  $I_5$  line shown in Fig. 3, except for the value of  $\rho_c$ ; i.e.,  $\rho_c \approx 0.5$  for the other  $I_i$  lines.

The peak positions of the Zeeman spectra for the  $I_i$  lines are plotted in Figs. 4(a) and 4(c) as functions of the magnetic field in  $\vec{H} \parallel c$  and  $\vec{H} \perp c$ , respectively. The angular,  $\theta_H$ , dependence of the peak positions is given in Fig. 4(b) for  $H = 7$  T.

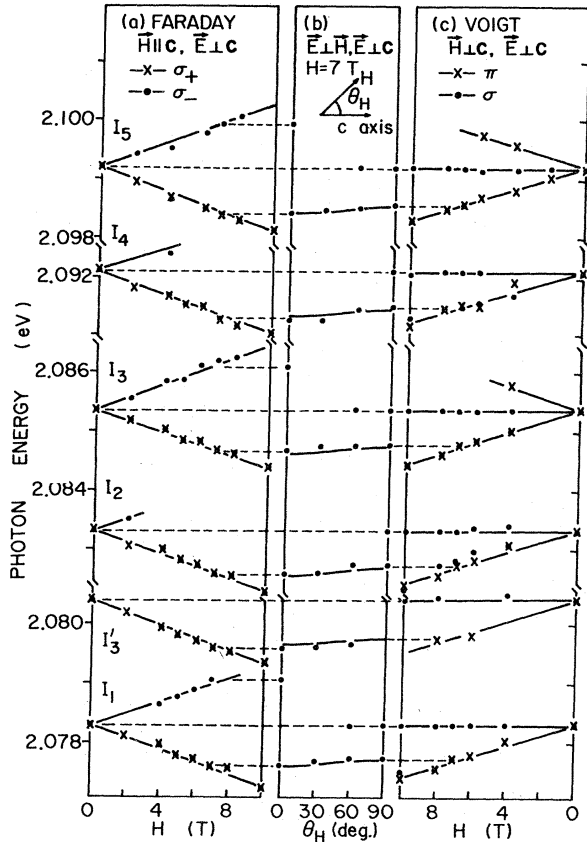


FIG. 4. (a) and (c), Zeeman splittings of the  $I_i$  lines at 4.2 K plotted against the magnetic field, and (b) similar plot against the angle  $\theta_H$  between the external field and the  $c$  axis. The component of the highest energy is not resolved above some magnetic field due to the thermal relaxation to the lower sublevels. The solid lines show the Zeeman splitting of the triplet state of the ( $D^*$ , X) bound exciton with the use of the  $g$  values in Eq. (6) (see Sec. V A).

Figure 4 indicates that the  $I_i$  lines split linearly into two and three for  $\vec{H} \parallel c$  and  $\vec{H} \perp c$ , respectively. If we express the energy separation of the outer two peaks as  $g\mu_B H$ , where  $g$  is the effective  $g$  value and  $\mu_B$  the Bohr magneton, the value of  $g_{\parallel}$  (for  $\vec{H} \parallel c$ ) or  $g_{\perp}$  (for  $\vec{H} \perp c$ ) is common to all the  $I_i$  lines with  $g_{\parallel} = 3.65 \pm 0.10$  and  $g_{\perp} = 3.23 \pm 0.15$ . The Zeeman splittings shown by the solid straight lines in Figs. 4(a) and 4(c) indicate that the diamagnetic shift may be neglected.

The  $\theta_H$  dependence of the peak positions shown in Fig. 4(b) indicates that the two components observed in  $\vec{H} \parallel c$  are connected smoothly to the outer two lines in  $\vec{H} \perp c$ , but the higher-energy branch of the two components is much weaker than the lower one due to the thermalization between the split states. The polarizations of the

outer two lines change from  $\sigma$  dominant to  $\pi$  dominant as  $\theta_H$  increases from 0 to 90°. The solid lines in Fig. 4(b) indicate the  $\theta_H$  dependence of the energy positions of the lowest component at  $H = 7$  T for the continuous change in the  $g$  value as

$$g = (g_{\parallel}^2 \cos^2 \theta_H + g_{\perp}^2 \sin^2 \theta_H)^{1/2}. \quad (1)$$

The central peak in  $\vec{H} \perp c$  with  $\sigma$  polarization disappears as  $\theta_H$  decreases from 90 to 0°, while its peak position does not change. The Zeeman spectra of the momentum-conserving phonon replica of the  $I_1$  to  $I_3$  lines were identical to the spectra of their zero-phonon lines described above.

### B. Temperature dependences

Figure 5 shows the temperature dependences of the integrated intensity of the  $I_i$  lines. The intensity  $I(T)$  at temperature  $T$  is approximated by

$$I(T) = I(0) / [1 + C \exp(-\Delta E/kT)], \quad (2)$$

where  $I(0)$  is the intensity at  $T = 0$ ,  $C$  a constant,  $\Delta E$  the thermal activation energy, and  $k$  the Boltzmann constant. Table I shows the energy position,  $\Delta E$ , and the optical binding energy ( $E_B^0$ ) of the  $I_i$  lines for a number of samples, where the optical binding energy is the energy difference between the indirect exciton (2.100 eV) and the  $I_i$  line. The table also summarizes the ionization energy of the binding center as estimated in Sec. V B.

## V. DISCUSSIONS

There are five kinds of bound-exciton states classified as follows according to the charged

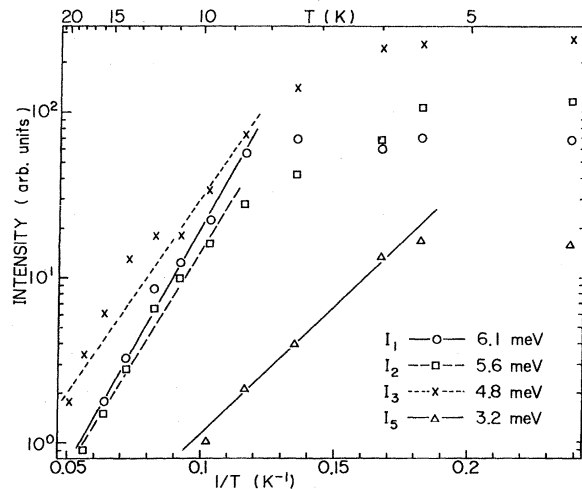


FIG. 5. Temperature dependences of the integrated luminescence intensity of the  $I_i$  lines. The activation energies deduced from the straight lines are also given in the figure.

TABLE I. The energy position, thermal activation energy ( $\Delta E$ ), and optical binding energy ( $E_B^0$ ) of the  $I_i$  lines and the ionization energy of the binding center.

| Line  | Energy position  | $E_B^0$ <sup>a</sup> (meV) | $\Delta E$ (meV) | Ionization <sup>b</sup> |
|-------|------------------|----------------------------|------------------|-------------------------|
|       | (meV)            |                            |                  | energy (meV)            |
| $I_1$ | $2078.5 \pm 0.4$ | $21.5 \pm 2.4$             | $5.5 \pm 1$      | 56                      |
| $I_2$ | $2083.2 \pm 0.4$ | $16.8 \pm 2.4$             | $4.1 \pm 1$      | 54                      |
| $I_3$ | $2085.5 \pm 0.4$ | $14.5 \pm 2.4$             | $4.5 \pm 0.5$    | 50                      |
| $I_5$ | $2099.2 \pm 0.4$ | $0.8 \pm 2.4$              | $3.3 \pm 0.2$    | 38                      |

<sup>a</sup>With the use of the indirect exciton energy of 2.100  $\pm$  0.002 eV.

<sup>b</sup>With the use of the indirect band-gap energy of 2.140 eV.

state of the binding center: (i) neutral donor ( $D^0, X$ ), (ii) neutral acceptor ( $A^0, X$ ), (iii) ionized donor ( $D^+, X$ ), (iv) ionized acceptor ( $A^-, X$ ), and (v) isoelectronic impurity ( $I, X$ ). One can distinguish the type of the binding center in the Zeeman spectra corresponding to the spin state of the binding center. The ( $D^0, X$ ) state, for example, consists of two electrons and one hole while ( $D^+, X$ ) consists of one electron and one hole. On the other hand, the temperature dependence of the luminescence intensity also gives the information on the type of binding center because the thermally released particle is an exciton for ( $D^0, X$ ) and ( $A^0, X$ ), while it is a hole (or an electron) for ( $D^+, X$ ) [or ( $A^-, X$ )], respectively.<sup>20</sup> One can analyze the present results according to the above-mentioned principles.

#### A. Zeeman analyses

In the present section a qualitative argument is given for identifying whether the binding center of IBE is an acceptor or an  $M$ -point donor. We also consider whether the impurity center is ionized or neutral. Since the separation between the bottom of the  $M$ -point conduction band ( $M_2^c$ ) and the second-lowest one ( $M_1^c$ ) is larger than the ionization energies of the  $M$ -point shallow donors by a factor of 10,<sup>9</sup> the shallow  $M$ -point donor states may consist mainly of the  $M_2^c$  wave function. There are three equivalent  $M$  valleys (symmetry  $C_{2v}$ ) in  $\epsilon$ -GaSe.<sup>13</sup> Hence, the donor level may show a valley-orbit splitting. The site symmetry of substitutional impurity is  $C_{3v}$ , and that of the interstitial impurities is  $D_{3h}$  or  $C_{3v}$  depending on the position of the impurity atom. The valley-orbit states of the  $M$ -point donors associated with  $M_2^c$ , therefore, are written as

$$A_1 + E (C_{3v})$$

or

$$A_2'' + E'' (D_{3h}).$$

If the  $I_i$  lines are related to the doubly degenerate  $E$  (or  $E''$ ) donor state, each line splits into eight or four in a magnetic field depending on the relative magnitude of the exchange energy of the electron and hole compared with the thermal energy  $kT$ . Experimental results shown in Figs. 3 and 4, however, indicate that the  $I_i$  line splits into three. The binding center responsible for the  $I_i$  lines, therefore, can not be attributed to the valley-orbit  $E$  (or  $E''$ ) state of the  $M$ -point donor.

The possibility of an exciton-acceptor complex is ruled out by the following reason, in addition to the energetic considerations given in Sec. V B: The valley-orbit splitting energy should be very small in the  $\Gamma$ -point acceptor complex since the orbital radius of the bound electron is very large due to the repulsive force between the acceptor core and the electron.<sup>21</sup> A multiplet structure, therefore, is expected for the exciton-acceptor complex, whereas no such structure is observed for the  $I_i$  line. The preceding discussions suggest that the binding center responsible for the  $I_i$  lines is the  $A_1$  (or  $A_2''$ ) valley-orbit state of the  $M$ -point donor. The donor levels at the  $M$ -point is expected to be lower than those at  $\Gamma$  in spite of the fact that the indirect gap ( $E_g^i$ ) is greater than the direct gap ( $E_g^d$ ) since the effective mass of the  $M$ -point conduction band is larger than that of the  $\Gamma$  point.<sup>22</sup>

The next problem is to identify whether the binding center is neutral or ionized from the Zeeman data. The Zeeman splitting of a ( $D^0, X$ ) complex is shown in Fig. 6(a) schematically,<sup>4</sup> where  $g_e$  and  $g_h$  are the effective  $g$  value of electron and hole, respectively. Figure 6(a) indicates that the ( $D^0, X$ ) line splits into two paired lines

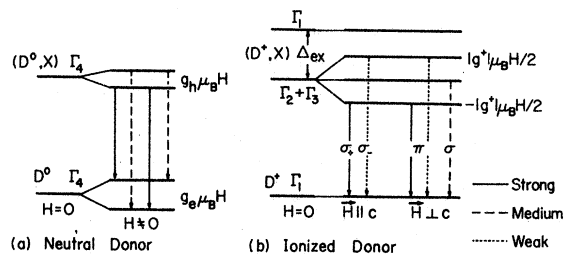


FIG. 6. Zeeman splittings of the valley-orbit  $A_1$  state of the bound excitons in the  $C_{3v}$  site symmetry and the selection rule for the optical transition. The relative luminescence line intensity is shown assuming (a)  $|g_h| \mu_B H \approx kT$  for ( $D^0, X$ ) and (b)  $|g^*| \mu_B H \approx kT$  for ( $D^+, X$ ) complexes, where  $g^* = g_e \pm g_h$ . Since  $\Delta_{ex} \gg kT$  and  $\Delta_{ex} \gg |g^*| \mu_B H$ , the effect of the spin singlet  $\Gamma_1$  state is negligible in ( $D^+, X$ ).

with separations of  $|g_e \pm g_h| \mu_B H$  in the magnetic field, while the  $I_i$  lines split into three. The  $(D^0, X)$  line may split into three apparently when  $g_e \simeq g_h$ , but the luminescence intensity of the line at  $-|g_e + g_h| \mu_B H/2$  must be equal to or weaker than the line at  $\pm |g_e - g_h| \mu_B H/2 \simeq 0$  independent of the magnitude of  $H$  for  $\vec{H} \perp c$ . In contrast with this prediction, the experimental result of Fig. 3 shows that among the three Zeeman subcomponents the one at the lowest energy is strongest, the central one is medium, and the one at the highest energy is weakest for  $\vec{H} \perp c$ . Hence, the bound state responsible for  $I_i$  are not  $(D^0, X)$ . The observed Zeeman spectra can be interpreted by ascribing the binding center to an ionized donor.

The electron in this  $(D^+, X)$  state belongs to the valley-orbit  $A_1$  (or  $A_2''$ ) state as discussed above. The symmetries of the electron and hole are  $\Gamma_4$  in the case of  $C_{3v}$  site symmetry. The bound-exciton state may split into  $\Gamma_4 \times \Gamma_4 = \Gamma_1 + \Gamma_2 + \Gamma_3$ . The basis functions for these states can be written in the band scheme given in Sec. II as

$$\begin{aligned} \Gamma_1(z): & (\phi_+^c \phi_+^v - \phi_-^c \phi_-^v) / \sqrt{2}, \\ \Gamma_2: & (\phi_+^c \phi_+^v + \phi_-^c \phi_-^v) / \sqrt{2}, \\ \Gamma_3(x): & (\phi_+^c \phi_+^v + \phi_-^c \phi_-^v) / \sqrt{2}, \\ \Gamma_3(y): & (\phi_+^c \phi_+^v - \phi_-^c \phi_-^v) / \sqrt{2}, \end{aligned} \quad (3)$$

where

$$\begin{aligned} \phi_+^c &= \alpha_e Z, \quad \phi_-^c = \beta_e Z, \\ \phi_+^v &= [\alpha_v + \gamma \beta_v (X + iY) Z / \sqrt{2}] / (1 + \gamma^2)^{1/2}, \\ \phi_-^v &= [\gamma \alpha_v (X - iY) Z / \sqrt{2} - \beta_v] / (1 + \gamma^2)^{1/2}, \end{aligned} \quad (4)$$

where  $\phi^c$  or  $\phi^v$  indicates the wave function of electron in the conduction or valence band, respectively  $(X \pm iY) Z / \sqrt{2}$  or  $Z$  the orbital part of the wave function,  $\alpha$  or  $\beta$  the spin function of electron and  $|\gamma| \simeq 0.1$  the mixing parameter of the  $p_{x,y}$ -like  $\Gamma_5^v$  band with the uppermost  $\Gamma_1^v$  band by the spin-orbit interaction.<sup>23</sup> In Eq. (3) the notations  $x$ ,  $y$ , and  $z$  in the parentheses show the direction of the dipole moment. If  $\gamma = 0$  the  $\Gamma_1$  and  $\Gamma_3$  bound exciton states are spin singlet and  $|S_z| = 1$  triplet states, respectively, but they are not purely singlet nor triplet due to the weak  $\Gamma_1^v$ - $\Gamma_5^v$  interband mixing. The  $\Gamma_2$  state, however, is a pure triplet. The exchange splitting energy,  $\Delta_{\text{ex}}$ , between the singlet  $\Gamma_1$  and triplet  $\Gamma_2 + \Gamma_3$  states may be several meV in an analogy with the direct exciton. The zero-field splitting between the  $\Gamma_2$  and  $\Gamma_3$  states has been estimated to be 0.016 meV from the recent experiments of the optically

detected magnetic resonance<sup>5</sup> and of the magnetic circular dichroism.<sup>7</sup>

The matrix for the linear Zeeman interaction is written as

| $\Gamma_1$           | $\Gamma_2$                      | $\Gamma_3(x)$                  | $\Gamma_3(y)$                    |
|----------------------|---------------------------------|--------------------------------|----------------------------------|
| $\Delta_{\text{ex}}$ | $g_{\parallel}^- \mu_B H_x / 2$ | $-i g_{\perp}^- \mu_B H_y / 2$ | $g_{\perp}^- \mu_B H_x / 2$      |
|                      | 0                               | $g_{\perp}^+ \mu_B H_x / 2$    | $-i g_{\perp}^+ \mu_B H_y / 2$   |
|                      | c.c.                            | 0                              | $-g_{\parallel}^+ \mu_B H_x / 2$ |
|                      |                                 |                                | 0, (5)                           |

where c.c. means the complex conjugate, subscripts  $\parallel$  and  $\perp$  indicate the direction of  $H$  with respect to the  $c$  axis, and  $g^{\pm} = g_e \pm g_h$ . In Eq. (5), the small zero-field splitting between  $\Gamma_2$  and  $\Gamma_3$  is neglected. Since  $\Delta_{\text{ex}} \gg |g^- \mu_B H|$  within the magnetic field of our experiment,  $H < 10$  T, the interaction between  $\Gamma_1$  and  $\Gamma_2 + \Gamma_3$  can be neglected. We obtain, therefore, the Zeeman splitting of the bound-exciton state by solving the  $3 \times 3$  matrix. The  $\Gamma_1$  state is not affected by the magnetic field in this approximation. Figure 6(b) shows a schematic of the Zeeman splitting deduced from Eq. (5). Except for the symmetry, the Zeeman splitting of the direct exciton or that of the bound exciton of the  $A_2''$  valley-orbit state in the  $D_{3h}$  site symmetry is identical to Fig. 6(b). The Zeeman splitting shown in Fig. 6(b) agrees with the experimental results shown in Figs. 3 and 4 in the number and the polarization of the split lines, although the observed lines are depolarized slightly.

Since  $\Delta_{\text{ex}} \gg kT$ , at least in the temperature range of  $T < 10$  K, the luminescence from the  $\Gamma_1$  state may not be observed. The peak positions of the outer two components in an arbitrary direction of the magnetic field are given by the effective  $g$  value of Eq. (1). The central one in the triplet state does not shift by the application of  $H$  for an arbitrary direction of  $H$ . The calculated  $\theta_H$  dependence of the peak positions agrees with the experimental result as shown in Fig. 4(b). Fig. 4(b).

The effective  $g$  values of the electron and hole are deduced to be

$$|g_{e\parallel} + g_{h\parallel}| = 3.65 \pm 0.1, \quad |g_{e\perp} + g_{h\perp}| = 3.23 \pm 0.15. \quad (6)$$

If one uses the estimation of  $g_{h\parallel} = 1.72$  by Morigaki *et al.*,<sup>5</sup>  $g_{e\parallel}$  of the donor electron is calculated to be 1.93, which is larger than the  $g$  value of 1.13 for the  $\Gamma$ -point electron.<sup>5</sup> Instead of  $g_{e\parallel} = 1.93$  for the donor electron it could be  $-5.37$  from Eq. (6), but the latter value seems to be improbable. The ratio of the spin relaxation time  $T_1$  to the lifetime  $\tau$  for the bound exciton may be deduced from the relative intensities of the  $S_z = \pm 1$  lines in  $\vec{H} \parallel c$ .

It was found for all the  $I_i$  lines that  $T_1 \approx \tau$ , where  $\tau$  is reported to be about  $10^{-6}$  sec.<sup>2,24</sup>

The Zeeman spectra for the  $(I, X)$  lines are expected to be identical to those of  $(D^+, X)$  given above since both complexes consist of one electron and one hole. Hence, one can not assign the binding center uniquely from the Zeeman data alone. The two kinds of complexes, however, may be distinguished in the case of indirect-gap materials from the phonon replica spectrum because the phonon replicas of  $(I, X)$  lines consist of the local mode phonons or they reflect the phonon density of states,<sup>25</sup> in contrast to  $(D^+, X)$  lines whose phonon replicas consist mainly of the momentum-conserving phonons. Since the momentum-conserving phonons contribute to the phonon replicas of the  $I_1$ ,  $I_2$ , and  $I_3$  lines,<sup>19</sup> the bound states responsible for these lines are not  $(I, X)$  but  $(D^+, X)$  complex.

The  $g$  value for the  $(I, X)$  complex may be different from that for  $(D^+, X)$  because the electron (or hole) wave function is highly localized at the iso-electronic center while it extends around shallow donor or acceptor centers.<sup>26</sup> The rest of the  $I_i$  lines ( $I'_3, I_4$ , and  $I_5$ ), therefore, are also attributed to  $(D^+, X)$  since the effective  $g$  value is common for all the  $I_i$  lines

#### B. Thermal quenching of the $I_i$ lines

The thermal activation energy of the luminescence intensity of bound excitons is equal to the optical binding energy for  $(D^0, X)$  or  $(A^0, X)$ , whereas it is not so for  $(D^+, X)$  or  $(A^-, X)$ . This discrepancy comes from the difference in the liberated particle by thermal excitation as interpreted at the beginning of this section. The thermal activation energies of the luminescence intensity of the  $I_1$  to  $I_3$  lines are, as shown in Table I, 20% to 30% of the optical binding energies. The bound states responsible for the  $I_i$  lines, therefore, are attributed to  $(D^+, X)$  or  $(A^-, X)$ .

Since the  $(D^+, X)$  [or  $(A^-, X)$ ] line is observed at<sup>20</sup>

$$E_g - E_D \text{ (or } E_A) - \Delta E,$$

one can estimate  $E_D$  (or  $E_A$ ) from the thermal quenching data, where  $E_D$  (or  $E_A$ ) and  $\Delta E$  are the ionization energy of the donor (or acceptor) and the thermal activation energy of the luminescence intensity, respectively. One may find from Table I that  $\Delta E$  is 3.3 to 5.5 meV and  $E_D$  (or  $E_A$ )  $\approx$  40 to 55 meV for the  $I_1$  to  $I_3$  and  $I_5$  lines assuming  $E_g^I = 2.140$  eV, whereas the ionization energies of the effective-mass acceptors are about 100 meV in  $\epsilon$ -GaSe.<sup>27</sup> Hence, the analysis of the temperature dependences of the  $I_i$  lines leads to the assignment that they originate from  $(D^+, X)$  with the donor ionization energy of 40 to 55 meV. This

assignment agrees with the conclusion of the Zeeman analyses.

The ratio,  $\Delta E/E_D$ , is about 0.1 for the lines of  $I_1$  to  $I_3$  and  $I_5$ . This ratio is larger than those for  $(D^+, X)$  complex in II-VI compounds, where  $\Delta E/E_D \approx 0.05$ .<sup>28</sup> One may calculate  $E_D$  with the use of the effective mass of electron at the  $M$  point as obtained from the transport experiments.<sup>22</sup> The calculated value is 112 meV in contrast with the above-mentioned value of about 50 meV. The discrepancy in  $E_D$  for the  $M$ -point donors suggests that the effective mass of the electron in Ref. 22 may be overestimated.

#### VI. CONCLUSIONS

The six PL lines due to the indirect bound exciton, called  $I_i$  lines, in the photon energy range from 2.0785 to 2.0992 eV in  $\epsilon$ -GaSe have been investigated by magnetoluminescence measurements up to 10 T and also by the temperature dependence of the PL spectrum in absence of a magnetic field. All the  $I_i$  lines show the same temperature and magnetic field dependences except for a slight variation in the thermal activation energy of the luminescence intensity, depending on the luminescence line.

The analyses of the Zeeman spectra and the thermal quenching data lead to the same conclusion that the binding centers responsible for the  $I_i$  lines are ionized donors. Furthermore, the spin and the valley-orbit states have been derived from the Zeeman data. The spin-triplet state is responsible for the  $I_i$  lines, where slight mixing of the singlet component due to the spin-orbit interaction makes the triplet states weakly allowed for  $\vec{E} \perp c$ . The valley-orbit state of the bound electron is assigned as  $A_1$  or  $A_2''$  in the site symmetry of  $C_{3v}$  or  $D_{3h}$ , respectively.

The effective  $g$  value of the  $M$ -point donor electron and that of the hole are  $|g_{e\parallel} + g_{h\parallel}| = 3.65 \pm 0.1$  and  $|g_{e\perp} + g_{h\perp}| = 3.23 \pm 0.15$ . Using the  $g$  value of the hole derived from the optically detected magnetic resonance,<sup>5</sup>  $g_{e\parallel}$  of the donor electron is calculated to be  $1.93 \pm 0.1$ .

The thermal quenching data of the  $I_i$  lines indicate that the ionization energy of the  $M$ -point donor is in the range of 40 to 55 meV. The binding energy of the hole to the neutral donor is about 10% of the ionization energy of the donor.

#### ACKNOWLEDGMENTS

The authors would like to thank K. Yamaguchi for his assistance in the experiments. One of the authors (Y.S.) would like to acknowledge the Sakkokai Foundation for financial support. This work was supported in part by the Grant-in-Aid for Scientific Research from the Ministry of Education in Japan.

- \*Present address: Department of Physics, University of California, Irvine, CA 92717. Permanent address: Tohoku University.
- <sup>1</sup>J. P. Voitchovsky and A. Mercier, *Nuovo Cimento* **22B**, 273 (1974).
- <sup>2</sup>N. Kuroda and Y. Nishina, *Phys. Status Solidi B* **72**, 81 (1975).
- <sup>3</sup>H. Serizawa, Y. Sasaki, and Y. Nishina, *J. Phys. Soc. Jpn.* **48**, 490 (1980).
- <sup>4</sup>D. G. Thomas and J. J. Hopfield, *Phys. Rev.* **128**, 2135 (1962).
- <sup>5</sup>K. Morigaki, P. Dawson, and B. C. Cavenett, *Solid State Commun.* **28**, 829 (1978).
- <sup>6</sup>Y. Sasaki and Y. Nishina, *J. Magn. Magn. Mater.* **11**, 143 (1979).
- <sup>7</sup>H. Anno and Y. Nishina, *Solid State Commun.* **29**, 439 (1979).
- <sup>8</sup>E. Mooser and M. Schlüter, *Nuovo Cimento* **18B**, 164 (1973).
- <sup>9</sup>M. Schlüter, J. Camassel, S. Kohn, J. P. Voitchovsky, Y. R. Shen, and M. L. Cohen, *Phys. Rev. B* **13**, 3534 (1976).
- <sup>10</sup>Y. Sasaki, C. Hamaguchi, and J. Nakai, *J. Phys. Soc. Jpn.* **38**, 162 (1975); **38**, 169 (1975).
- <sup>11</sup>F. Meyer, E. E. de Kluizenaar, and D. den Engelsen, *J. Opt. Soc. Am.* **63**, 529 (1973).
- <sup>12</sup>A. Balzarotti, M. Piacentini, E. Brauttini, and P. Picozzi, *J. Phys. C* **4**, L273 (1974).
- <sup>13</sup>M. Schlüter, *Nuovo Cimento* **13B**, 313 (1973).
- <sup>14</sup>G. F. Koster, J. O. Dimmock, R. G. Wheeler, and H. Statz, *Properties of the Thirty-Two Point Groups* (MIT Press, Cambridge, 1963).
- <sup>15</sup>N. Kuroda, I. Munakata and Y. Nishina, *Solid State Commun.* **33**, 687 (1980).
- <sup>16</sup>N. Kuroda and Y. Nishina, *J. Luminescence* **12/13**, 623 (1976).
- <sup>17</sup>A. Mercier, E. Mooser, and J. P. Voitchovsky, *Phys. Rev. B* **12**, 4307 (1975).
- <sup>18</sup>Le C. Thanh and C. Depeursinge, *Solid State Commun.* **21**, 317 (1977).
- <sup>19</sup>Y. Sasaki and Y. Nishina, unpublished. See also Ref. 3.
- <sup>20</sup>H. B. Bebb and E. W. Williams, in *Semiconductors and Semimetals*, edited by R. K. Willardson and A. C. Beer (Academic, New York, 1972), Vol. 8, p. 181.
- <sup>21</sup>P. J. Dean, R. A. Faulkner, S. Kimura, and M. Ilegems, *Phys. Rev. B* **4**, 1926 (1971).
- <sup>22</sup>G. Ottaviani, C. Canali, F. Nava, Ph. Schmid, E. Mooser, R. Minder, and I. Zschokke, *Solid State Commun.* **14**, 933 (1974).
- <sup>23</sup>The wave functions given in Eq. (3) are very similar to those of the *B* exciton in the wurtzite materials due to the similarity in the direct absorption edge of GaSe and the wurtzite materials. The difference in the wave functions between GaSe and the wurtzite materials comes from the appearances of the bonding and antibonding states between the wave functions of the two Se atoms in a unit cell. See also Refs. 13 and 15.
- <sup>24</sup>J. P. Voitchovsky and A. Mercier, *Phys. Status Solidi A* **18**, 545 (1973).
- <sup>25</sup>D. J. Wolford, B. G. Streetman, S. Lai, and M. V. Klein, *Solid State Commun.* **32**, 51 (1979).
- <sup>26</sup>P. J. Dean and R. A. Faulkner, *Phys. Rev.* **185**, 1064 (1969).
- <sup>27</sup>Ph. Schmid, J. P. Voitchovsky, and A. Mercier, *Phys. Status Solidi A* **21**, 443 (1974).
- <sup>28</sup>T. Skettrup, M. Suffczynski, and W. Gorzkowski, *Phys. Rev. B* **4**, 512 (1971).